# Optimized Mobile Retroreflectivity Unit Data Processing Algorithms

Final Report
Florida Department of Transportation
Contract Number: BDV 34 TWO# 977-03
April 2017

*Author:*

Fenner Colson
FDOT Materials Research Park
5007 NE 39th Ave.
Gainesville, FL 32609
(352) 955-9337
fenner.colson@dot.state.fl.us

*FDOT Contact:*

Joshua Sevearance
FDOT Materials Research Park
5007 NE 39th Ave.
Gainesville, FL 32609
(352) 955-6336
joshua.sevearance@dot.state.fl.us

*Principle Investigator:*

James H. Fletcher
University of North Florida
School of Engineering
Jacksonville, FL 32224
(904) 620-1844
jfletche@unf.edu

## DISCLAIMER

The opinions, finding, and conclusions expressed in this publication are those of the authors and not necessarily those of the State of Florida Department of Transportation.

**Metric Conversion Chart**

| Symbol | When you know | Multiply by | To find | Symbol |
|---|---|---|---|---|
| | | Length | | |
| in. | inches | 25.4 | millimeters | mm |
| ft | feet | 0.305 | meters | m |
| yd | yards | 0.914 | meters | m |
| mi | miles | 1.61 | kilometers | km |
| | | Area | | |
| $in^2$ | square inches | 645.2 | square millimeters | $mm^2$ |
| $ft^2$ | square feet | 0.093 | square meters | $m^2$ |
| $yd^2$ | square yard | 0.836 | square meters | $m^2$ |
| ac | acres | 0.405 | hectares | ha |
| $mi^2$ | square miles | 2.59 | square kilometers | $km^2$ |
| | | Volume | | |
| fl oz | fluid ounces | 29.57 | milliliters | mL |
| gal | gallons | 3.785 | liters | L |
| $ft^3$ | cubic feet | 0.028 | cubic meters | $m^3$ |
| $yd^3$ | cubic yards | 0.765 | cubic meters | $m^3$ |
| | | Mass | | |
| oz | ounces | 28.35 | grams | g |
| lb | pounds | 0.454 | kilograms | kg |
| T | short tons (2000 lb) | 0.907 | megagrams | Mg |
| | | Temperature | | |
| °F | Fahrenheit | $\frac{5}{9}(F-32)$ | Celsius | °C |
| | | Illumination | | |
| fc | foot-candles | 10.76 | lux | lx |
| fl | foot-Lamberts | 3.426 | $\frac{\text{candela}}{m^2}$ | $\frac{cd}{m^2}$ |
| | | Stress/Pressure | | |
| lbf | poundforce | 4.45 | newtons | N |
| $\frac{lbf}{in^2}$ (or psi) | $\frac{\text{poundforce}}{\text{square inch}}$ | 6.89 | kilopascals | kPa |

## Technical Report Documentation Page

| 1. Report No. | 2. Government Accession No. | 3. Recipient's Catalog No. |
|---|---|---|
| BDV 34 TWO# 977-03 | | |

| 4. Title and Subtitle | 5. Report Date |
|---|---|
| Optimized Mobile Retroreflectivity Unit Data Processing Algorithms | April 2017 |
| | 6. Performing Organization Code |
| 7. Author(s) | 8. Performing Organization Report No. |
| Fenner Colson, Joshua Sevearance, James H. Fletcher | |
| 9. Performing Organization Name and Address<br>University of North Florida<br>1 UNF Drive<br>Jacksonville, FL 32224 | 10. Work Unit No. (TRAIS) |
| | 11. Contract or Grant No. |
| 12. Sponsoring Agency Name and Address<br>Florida Department of Transportation<br>605 Suwannee Street<br>Tallahassee, Florida 32399-0450 | 13. Type of Report and Period Covered<br>Draft Final Report<br>June 2014 – April 2017 |
| | 14. Sponsoring Agency Code |

15. Supplementary Notes

16. Abstract

The University of North Florida, in collaboration with the FDOT, was tasked to establish precise line-stripe evaluation methods using the Mobile Retroreflectivity Unit (MRU). Initial implementation of the manufacturer's software resulted in measurements with inferior repeatability, where this loss in data quality was attributed to external factors, specifically raised pavement markers and discontinuous line striping. Mitigation of these on-road inputs was successfully completed ensuring quality MRU measurements of pavement marking reflectivity. New data processing algorithms were developed, tested, and optimized as part of the ongoing effort to mitigate on-road inputs and raise MRU performance standards.

| 17. Key Words | 18. Distribution Statement |
|---|---|
| Retroreflectivity, laser measurement, algorithm, optimization, repeatability, raised pavement markers, interference filters | |

| 19. Security Classif. (of this report) | 20. Security Classif. (of this page) | 21. No. of Pages | 22. Price |
|---|---|---|---|
| Unclassified | Unclassified | 40 | |

**Form DOT F 1700.7** (8-72)

## EXECUTIVE SUMMARY

The project team, University of North Florida researchers in collaboration with the FDOT personnel, successfully developed optimized data processing algorithms for the Mobile Retroreflectivity Unit (MRU). The new algorithms demonstrate 8.9% repeatability improvement with respect to the vendor's software. In order to implement the algorithms, an in-house software application was built, entitled Florida Retroreflectivity Software (FRS). This software is fully operational, and incorporates MRU control as well as data processing and provides enhanced capabilities to the operator.

The first step in the project was to fully understand the MRU response to line striping. The MRU sweeps a laser light in an approximately 1 meter arc and collects 1000 data points during the sweep. The 1000 data points are split into the following three categories: background, slew rate, and representative stripe data. This is done to ensure that only data that properly represents actual line striping retroreflectivity is used in the evaluation.

The data processing algorithms utilized the gradient method (identifying slopes of maximum and minimum value) to identify true stripe data. Spurious inputs, such as Raised Pavement Markers (RPMs), are easily identifiable and the resulting data removed from any further calculations. Optimization of the algorithms included investigation of different post-processing steps and integration of mitigation strategies, such as accounting for vehicle wander.

Extensive on-road testing was completed to help identify the root causes of loss in data repeatability. Part of the on-road testing included a repeatability study that showed improved data repeatability over the vendor-supplied software. The on-road testing indicated, at times, a shifting of the data upwards or downwards although the data trends were similar. One of the main benefits of the FRS software is that it provides a much more detailed insight into the MRU operation, and as a result, it is apparent that the level and direction of ambient light can significantly impact MRU performance.

The MRU includes interference filter hardware designed to block extraneous light (not at the frequency of the laser light). Testing has showed that the performance of this sub-system is often insufficient. Many factors, such as temperature and age, can affect the interference filter performance and further testing is on-going to better understand the limitation of this hardware. Once completed, additional mitigation strategies can be incorporated into the FRS to further improve data repeatability.

TABLE OF CONTENTS

Disclaimer ..... ii
Metric Conversion Chart ..... iii
Technical Report Documentation Page ..... iv
Executive Summary ..... v
List of Figures ..... viii
List of Tables ..... ix
1. Background ..... 1
2. Initial Data Collection ..... 1
2.1. Background Voltage ..... 1
2.2. Slew Rate ..... 2
2.3. Stripe Data ..... 3
3. Signal Characteristics ..... 3
3.1. Low Stripe Reflectivity ..... 3
3.2. RPM Signal ..... 4
3.3. Partial RPM Signal ..... 4
3.4. Excessive $R_L$ Signal ..... 5
3.5. Double Stripe ..... 5
4. Algorithm Development ..... 6
4.1. Gradient Method ..... 6
4.2. Calibration ..... 8
4.3. Algorithm Optimization ..... 10
4.3.1. Scan Bounding ..... 10
4.3.2. Stripe Splitting ..... 11
4.3.3. Fourier Analysis ..... 12
4.3.4. Lateral Wander Correlation ..... 15
4.4. Implementation Software ..... 16
5. On-Road Testing and Debugging ..... 19
5.1. Power Supply Inconsistency ..... 19
5.2. Background Light Effects ..... 20
5.3. Voltage Offset ..... 21
5.3.1. Histogram Analysis ..... 22

5.4. Spinning Mirror Assembly Effects ..... 23
6. Repeatability Study ..... 24
7. Conclusions and Future Work ..... 29
Glossary ..... 30
References ..... 31

List of Figures

Figure 1: Signal characteristics of a reflecting stripe. 2
Figure 2: Slew rate and stripe width mixing. 2
Figure 3: Stripe voltage due to retroreflected laser light. 3
Figure 4: Example of low stripe signal. 4
Figure 5: Example of an RPM voltage signal. 4
Figure 6: Thin stripe signal due to glancing RPM reading. 5
Figure 7: Unrecognizable stripe waveform. 5
Figure 8: Identification of a double stripe. 6
Figure 9: Locate maximum and minimum gradients. 7
Figure 10: Locate stripe data boundaries. 7
Figure 11: Mean voltage over the stripe width. 8
Figure 12: Relationship between RL and voltage. 9
Figure 13: Flowchart of data extraction process. 9
Figure 14: Scan periphery optimization. 11
Figure 15: Stripe splitting optimization. 12
Figure 16: Data to analyze with Fourier technique. 13
Figure 17: Frequency space analysis. 13
Figure 18: High pass filter Fourier analysis. 14
Figure 19: Low pass filter Fourier analysis. 14
Figure 20: Band stop filter Fourier analysis. 15
Figure 21: Lab setup for lateral correlation derivation. 15
Figure 22: Curve fit establishing lateral correlation. 16
Figure 23: FRS (Top) and vendor software (Bottom) comparison. 17
Figure 24: Drop down menu options. 18
Figure 25: Sensor readout data. 18
Figure 26: Real time data spreadsheet. 19
Figure 27: Data using stable house power supply. 20
Figure 28: Data quality loss due to thermoelectric cooler. 20
Figure 29: Effect of solar orientation. 21
Figure 30: Example of vertical offset between runs. 22
Figure 31: Histogram analysis. 23
Figure 32: Variation due to spinning mirror instability. 24
Figure 33: Data from precision site 3 exhibiting superb repeatability. 25
Figure 34: Vertical offsetting at site 6. 26

List of Tables

Table 1: Algorithm optimization methods summary. 10
Table 2: Summary of repeatabilities at sites 1-5 (3 runs). 25
Table 3: Data collection at sites 6-8 (5 runs). 26
Table 4: Site 6-8 repeatability calculated under consistent ambient conditions (Run #2-4) 27

# 1. Background

Evaluation of pavement marking reflectivity has historically been accomplished via handheld retroreflectometers. The handheld retroreflectometers are sufficiently accurate but are limited in scope, since measurements characterize reflectivity at only a single location. Entire roadway striping often varies significantly in reflectivity, demanding higher spatial resolution. Using handheld retroreflectometers to acquire reflectivity measurements along hundreds of miles of state roadways is notably inefficient.

The FDOT assessed Mobile Retroreflectivity Units (MRUs) to determine the applicability of the technology for pavement reflectivity evaluation. Initial evaluation and optimization of the technology focused on improving the hardware. For example, a cooling system was integrated to existing MRU design to tightly control its operating temperature. Additionally, new calibration materials were tested and selected to establish an optimized, robust calibration process. The MRU technology demonstrated satisfactory performance and a statewide pavement marking evaluation program was implemented.

On-going evaluation of MRU repeatability and reproducibility indicated loss in data quality due to on-road inputs such as raised pavement markers (RPMs). Mitigation of the effects included operators adjusting for these inputs mid-testing, where manual control of data collection tended to worsen repeatability. Optimized algorithms to automatically process the data and mitigate on-road inputs were proposed to remove operator influence and maximize repeatability.

# 2. Initial Data Collection

The MRU acquires voltage signals from the amplified electrical response of a photodetector exposed to retroreflected laser light from on-road pavement markings. The amplified voltage signal is routed through NI data acquisition hardware to a computer USB connection where data can be saved and processed using LabVIEW software.

The MRU sweeps the laser light across an approximately one meter arc, during which the DAQ system collects 1000 data points of the resulting amplified voltage signal. These data points can be categorized into the following three primary characteristics: background voltage, slew rate, and stripe data. The data must be separated in an automated manner in order to successfully identify the data points related to the stripe reflectivity. See *Figure 1* for an illustration of these characteristics.

## 2.1. Background Voltage

MRU response includes reflected laser light from the roadway material (background) immediately surrounding the stripe, as seen in *Figure 1*. The amplitude of reflectivity is typically ~0.2 V but can vary slightly due to variation in roadway composition.

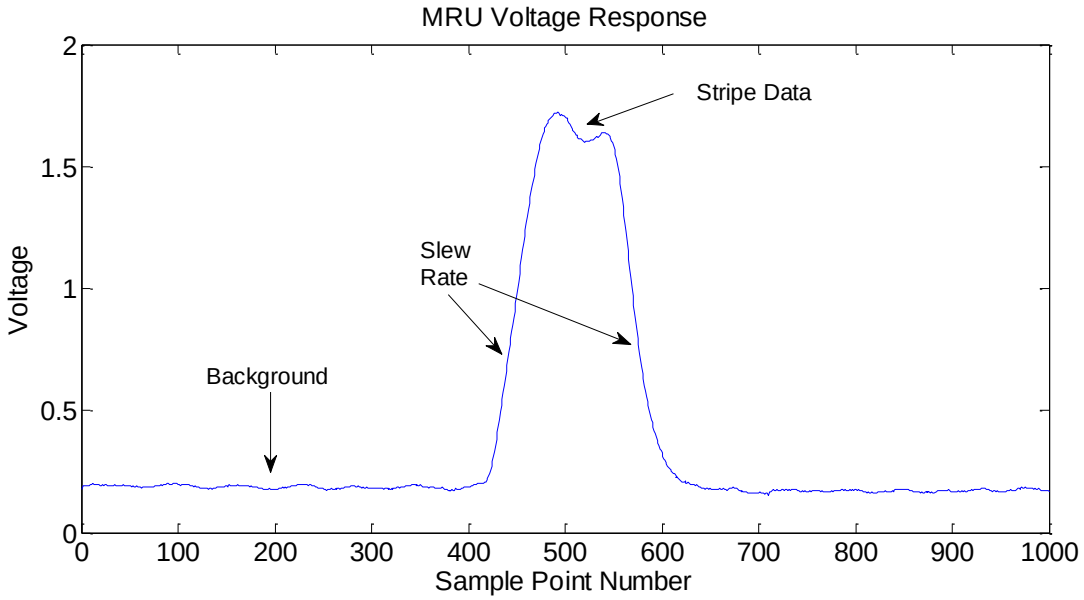


Figure 1: Signal characteristics of a reflecting stripe.

### 2.2. Slew Rate

At the moment of transition between background and stripe data, operational amplifier dynamics demand a finite response time, referred to as slew rate. Slew rate response time partially masks stripe data, specifically the first 2 inches of the physical stripe in the direction of laser sweep, see *Figure 2*. The retro-reflectivity of remaining portion of the stripe can be accurately measured since transient electrical response has recovered. As the laser light leaves the stripe and once again is hitting the background material the slew rate re-appears as the photodetector response returns to background voltage.

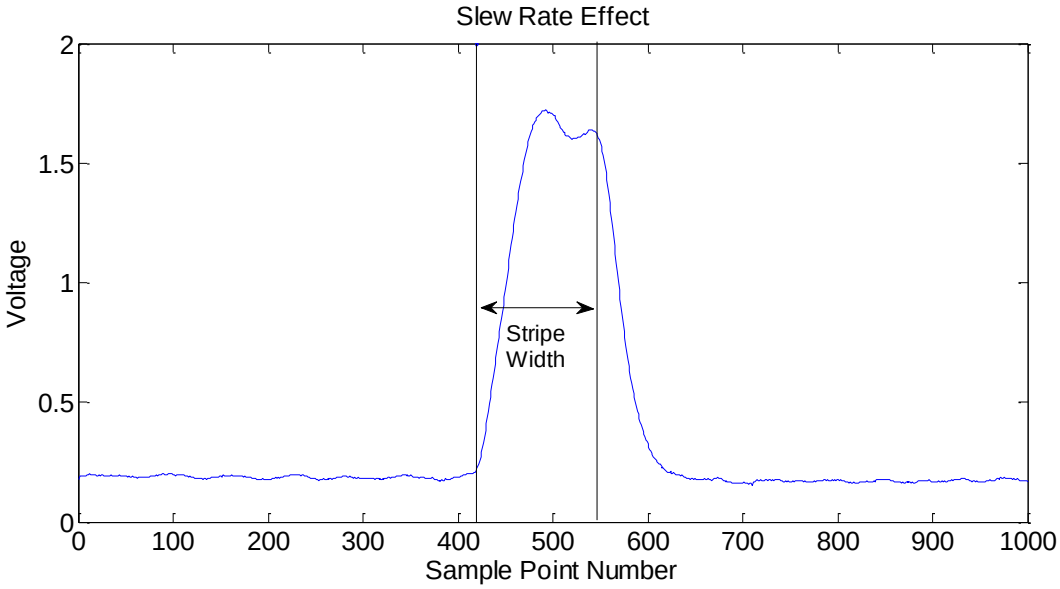


Figure 2: Slew rate and stripe width mixing.

### 2.3. Stripe Data

The plateau between the slew rate responses corresponds to retro-reflected laser light from the stripe. The data is not necessarily a flat plateau but can contain slight variations due to the non-uniform nature of the stripe material as shown in *Figure 3*. This voltage is a true characteristic of the stripe reflectivity and constitutes a measurement of retroreflected laser light.

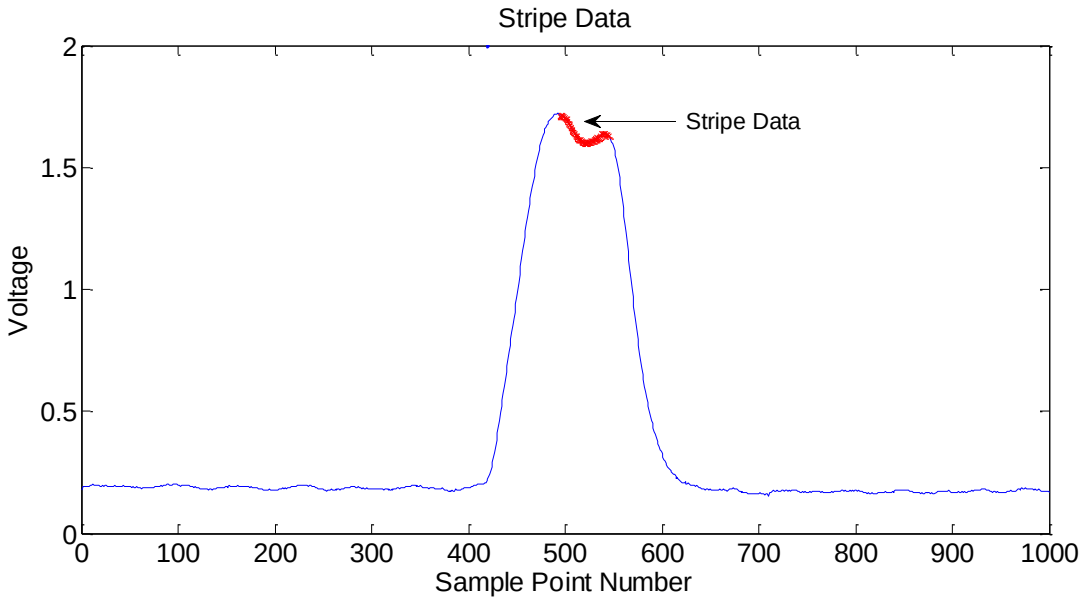


Figure 3: Stripe voltage due to retroreflected laser light.

## 3. Signal Characteristics

The shape of a stripe signal is very consistent in laboratory settings but varies considerably during on-road testing, often due to on-road inputs. Variability in the shape of the voltage response due to on-road inputs falls under one of the following categories: low stripe reflectivity, RPM signal, partial RPM signal, excessive $R_L$ signal, or double stripe. Each signal waveform can be identified as a response to a particular on-road input.

### 3.1. Low Stripe Reflectivity

On-road stripes characterized by low reflectivity (*Figure 4*) are difficult to identify since the difference between background voltage and stripe voltage is small. A minimum voltage level is set by the operator in order to ensure that the data is from the retro-reflectivity of a stripe. Any reading that falls below the minimum voltage level is flagged as low reflectivity data and removed from the data set used to evaluate tenth mile retro-reflectivity values for the line striping.

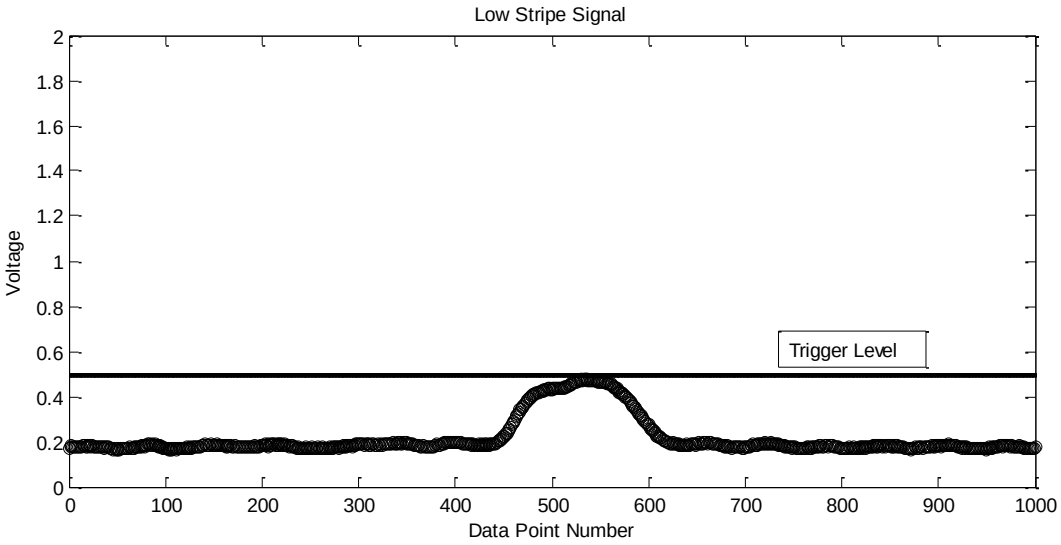


Figure 4: Example of low stripe signal.

### 3.2. RPM Signal

Raised pavement markers are highly reflective and result in saturating the photodetector to its maximum voltage allowed by the software. The signal can be identified by establishing a maximum RPM voltage level set by the operator, as seen in *Figure 5*. Whenever the signal rises above a maximum threshold voltage set by the operator, the data is flagged as an RPM reading and removed from the data set.

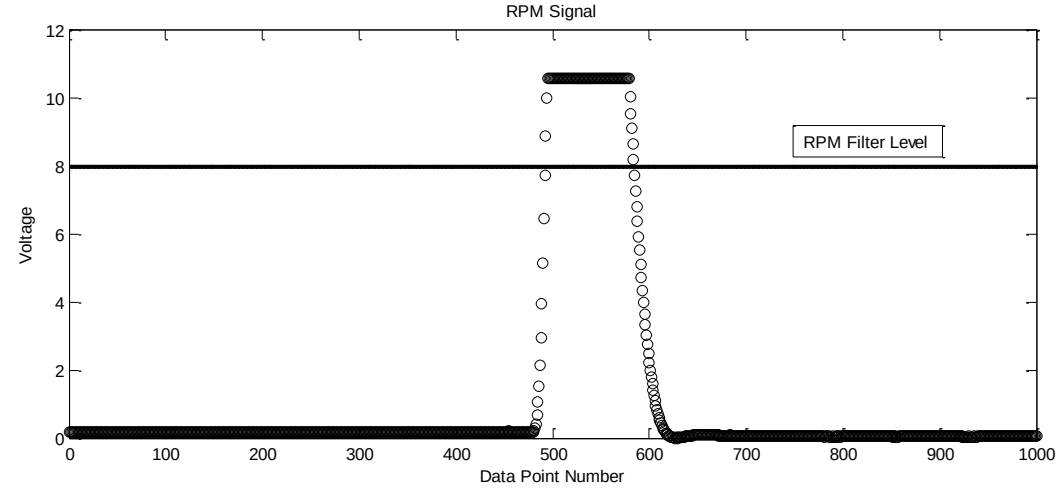


Figure 5: Example of an RPM voltage signal.

### 3.3. Partial RPM Signal

If during the one meter sweep, the laser light partially hits a raised pavement marker, the resulting voltage response resembles an exceptionally thin stripe (*Figure 6*). In contrast to a direct reflection from the RPM, the laser lands on only part of the RPM, and thus the full RPM waveform

(*Figure 5*) is not developed. As a result, the voltage remains low and does not reach the maximum level. Since on-road pavement stripe markings typically are 6 inches in width, such an input can be identified by recognizing the stripe's insufficient width, and removed from saved data.

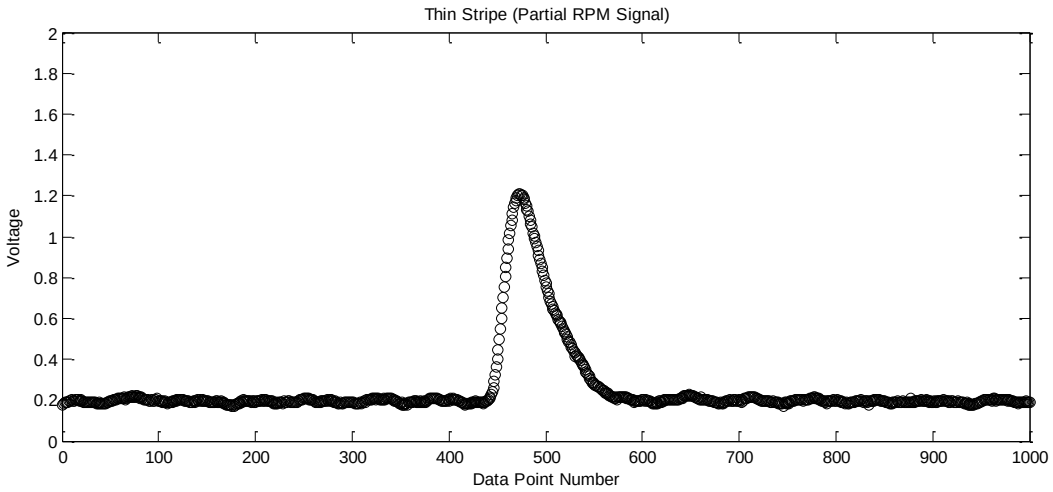


Figure 6: Thin stripe signal due to glancing RPM reading.

### 3.4. Excessive $R_L$ Signal

Various on-road inputs, such as stopbars, can register as excessive retroreflected laser light resulting in an unrecognizable stripe waveform (*Figure 7*). This type of data is automatically removed from saved data.

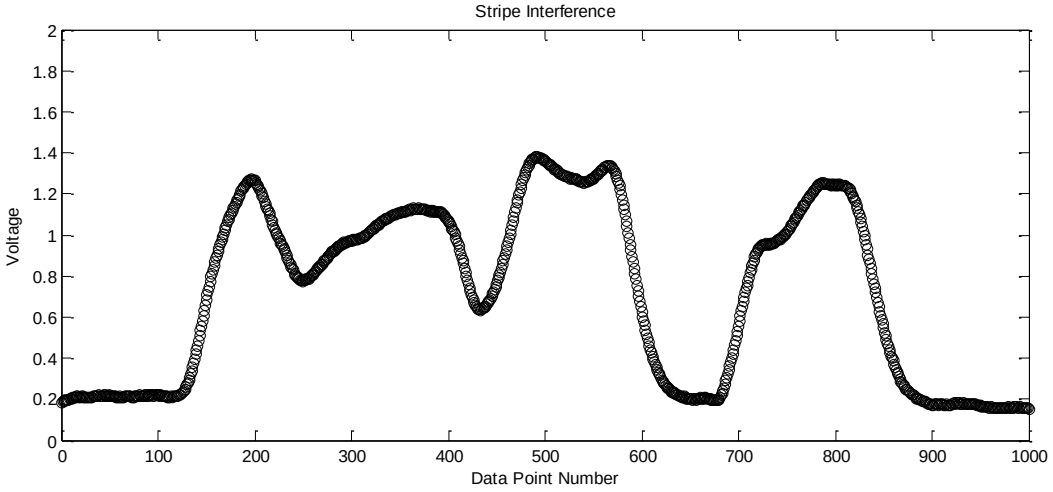


Figure 7: Unrecognizable stripe waveform.

### 3.5. Double Stripe

Double stripe signals apply the gradient method (see Section 4.1) to each stripe waveform instead of the entire scan. Data which crosses a trigger level four times instead of two (*Figure 8*)

is identified as a double stripe. Monitoring how many crossings determines whether or not to process the scan as a single stripe or a double stripe.

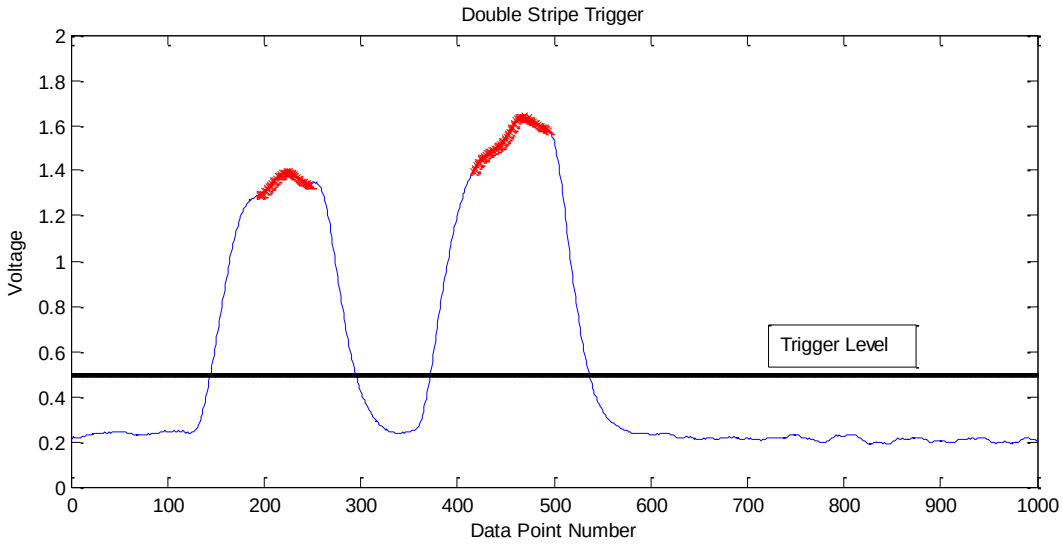


Figure 8: Identification of a double stripe.

# 4. Algorithm Development

## 4.1. Gradient Method

An automated computing process has been developed to efficiently and accurately separate useful stripe data from the entirety of the scan. Data analysis is completed immediately following the collection of a single measurement scan. The process takes advantage of the characteristic shape of the slew rate, specifically its rapid change in voltage, by calculating the gradient, i.e. the slope. Since the largest gradients always occur during the slew rate and at the same position relative to the stripe data, obtaining the location of the maximum and minimum gradient (*Figure 9*) is necessary to consistently identify stripe data.

Once the gradient extrema are identified, appropriate data point shifting identifies the beginning and end of data that accurately represents the stripe retroreflectivity data. The number of points to shift away from the gradient maximum or minimum was determined empirically by studying large amounts of data to determine the best values. These values are adjustable but the current default values are a 40 point shift to the right and a 25 point shift to the left from the maximum and minimum gradients, respectively (see *Figure 10*). Once the true stripe retro-reflectivity data points for each laser sweep has been identified, the data points are averaged into a single data point (mean voltage) as seen in *Figure 11*.

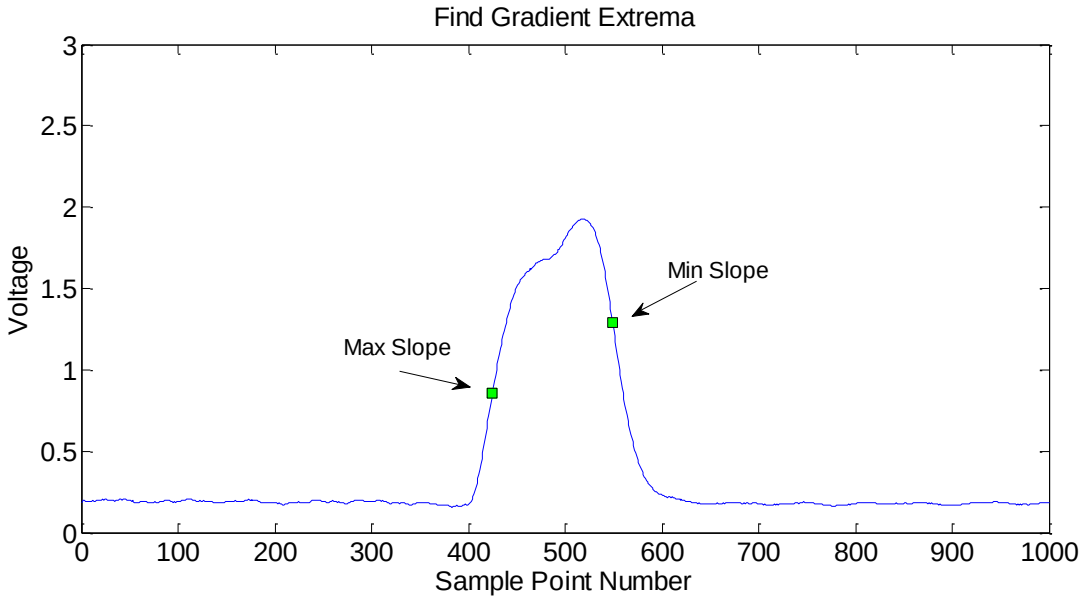


Figure 9: Locate maximum and minimum gradients.

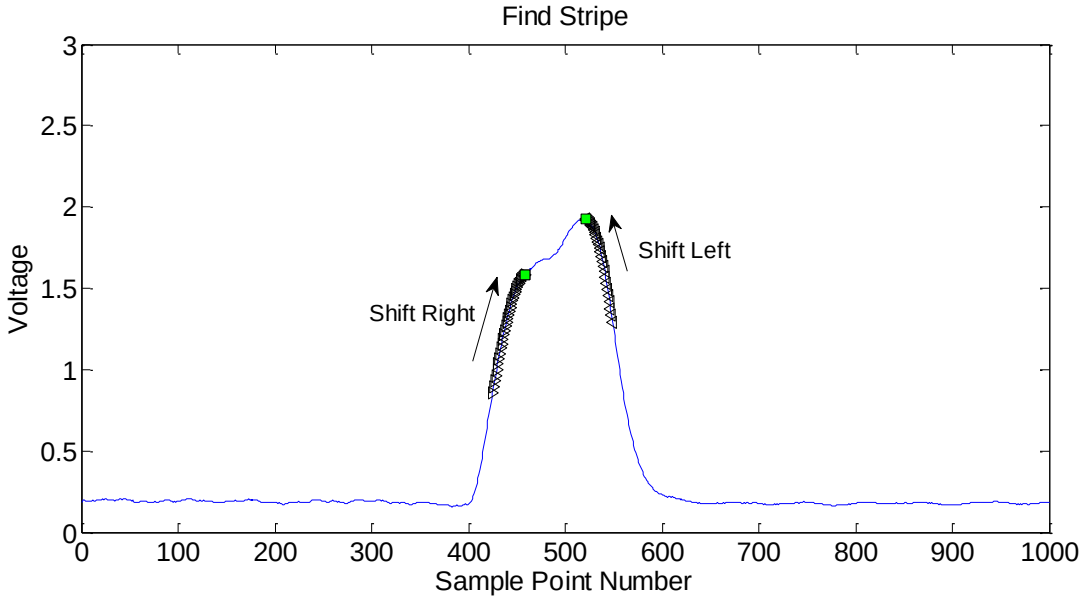


Figure 10: Locate stripe data boundaries.

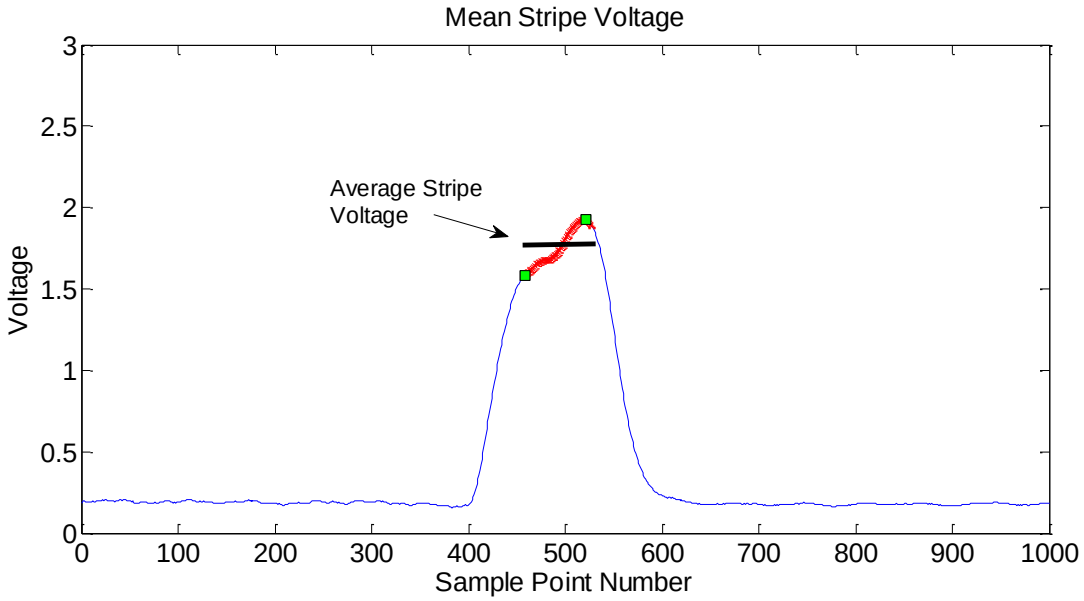


Figure 11: Mean voltage over the stripe width.

The algorithm process repeats at 20 Hz in sync with the rate at which data is acquired. If a stripe is not identified during the scan (either due to skip lines or spurious on-road inputs such as RPMs), the entire scan is flagged and not saved to the tenth mile calculations. If the scan contains a double stripe, the algorithm method is applied to each stripe waveform. The high level overview of algorithm behavior is summarized in *Figure 13*.

### 4.2. Calibration

The acquired signal is measured in units of volts, which is the output of the MRU photodetector and amplifier. The voltage signal is converted to units of retro-reflectivity (mcd/lux/m$^2$ or symbol $R_L$) through the calibration process. The conversion is completed by multiplying the voltage by a proportionality constant, i.e. the calibration factor. Verification of this proportionality was completed by measuring voltage response while directly reducing $R_L$ by adding neutral density filters in-line with the retroreflected laser light (*Figure 12*). Since the voltage response versus retroreflected light is a highly linear function ($R^2$ = 0.9971) that passes through the origin, a single calibration factor can be used to convert between the two units.

In practice, the calibration factor is established by measuring a vinyl sample with a known $R_L$ value (as determined by a photometric range). Since the relationship between voltage and $R_L$ is linear, a one-point calibration is sufficient across the entire range of on-road retroreflectivity.

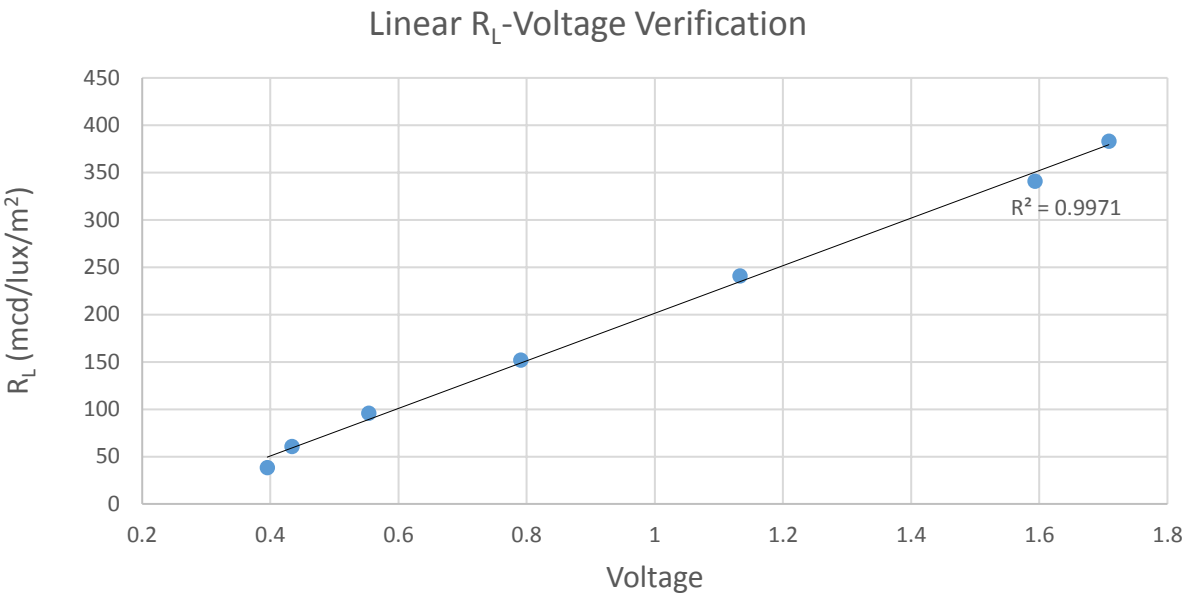


Figure 12: Relationship between RL and voltage.

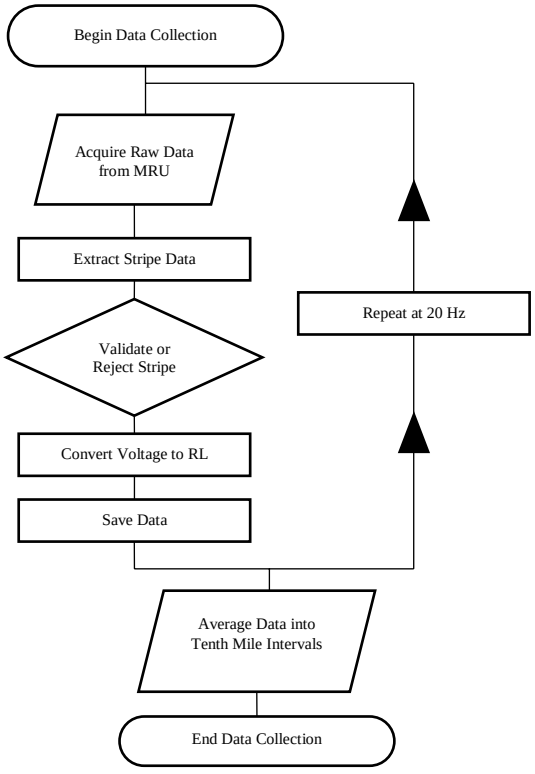


Figure 13: Flowchart of data extraction process.

### 4.3. Algorithm Optimization

Raw data is typically characterized by significant variation during on road testing and thus several methods were applied as part of the process to understand data variation and how it could be minimized. The methods applied are summarized in *Table 1* and are detailed in the following sections.

Table 1: Algorithm optimization methods summary.

| Optimization Method | Technique | Conclusion |
|---|---|---|
| Scan Bounding | Save data from partial subset of scan window | Maximize scan window (1000 points) |
| Stripe Splitting | Average stripe data over the first, second, and third portions of the stripe | Negligible effect |
| Fourier Analysis | Fourier transform data and filter out vehicle vibration frequencies | Negligible effect |
| Lateral Correlation | Adjust voltage data based on relative location in window | 4.7% point increase in repeatability |

#### *4.3.1. Scan Bounding*

As the laser sweeps its one meter arc, 1000 data points are collected. Ideally the stripe falls in the center of the one meter arc, but this is not always the case due to vehicle wander. Testing has shown that the measured retro-reflectivity for a stripe changes as the stripe location within the one meter arc changes, resulting in increased data variability. The effect of preferentially using only the data in the middle of the one meter sweep and eliminating the data points at the edges was optimized with respect to repeatability. Optimization was explored by varying the interval to include the whole window (1000 point scan interval) or shortening the window to only include the center 200 point interval. The results of testing showed that this approach did not significantly improve the repeatability, *Figure 14* shows how the best repeatability occurred when the entire 1000 point window was used. In shorter intervals, the repeatability worsened because too much data was eliminated and thus the tenth mile average was based on too few data points. As a result of this testing, the entire 1000 data points are used.

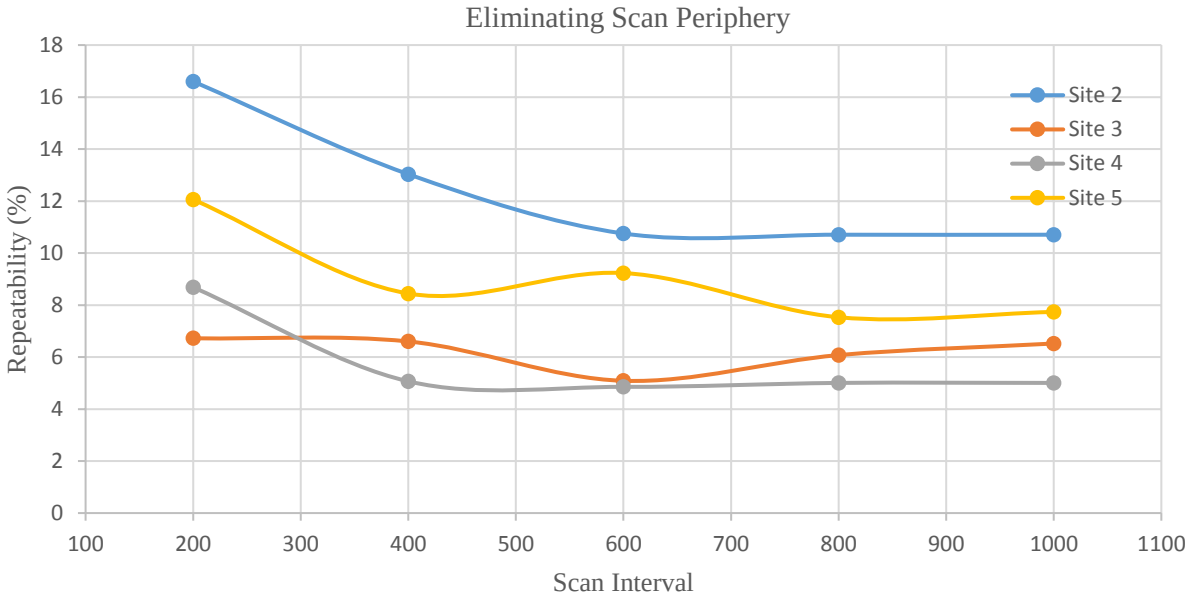


Figure 14: Scan periphery optimization.

### *4.3.2. Stripe Splitting*

An alternative to averaging stripe data across the width of the stripe was explored. Instead of calculating the mean voltage across the stripe width, data was averaged by a weighting function by its position on the stripe. Since stripes are asymmetrically more worn on the inside of the stripe, the intention was to explore if the weighting averaging technique could be optimized to take advantage of the asymmetry. For example, the laser scans can be organized into different segments. The first third of the stripe can be separated from the second and final third. Each portion of the stripe will have a different reflectivity since the portion of the stripe nearest to the road will be more worn than the portions that are farther away due to erosional effects from vehicles driving on the stripes. The method splits each stripe width into three parts and averages the three portions separately and subsequently averages each third into a single data point (see *Figure 15*). The test data showed this approach had a negligible effect on data variability.

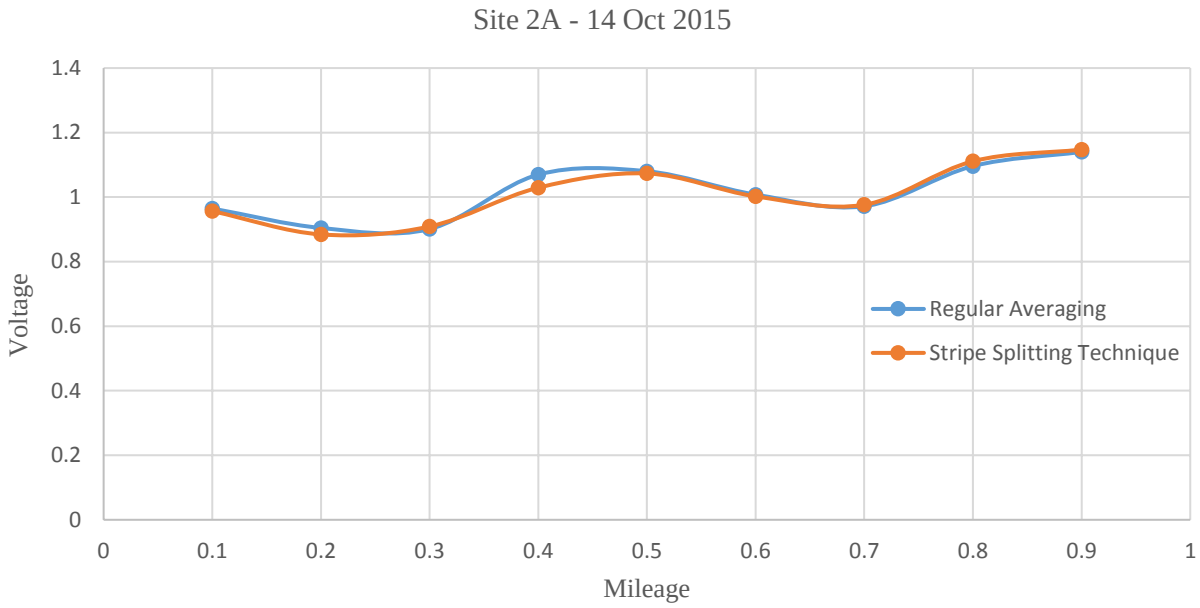


Figure 15: Stripe splitting optimization.

### *4.3.3. Fourier Analysis*

Data collected on-road often exhibited waveforms resembling periodic sinusoid waves, as illustrated in *Figure 16*. Fourier analysis of the data was explored in hopes of finding a hidden frequency which could be filtered out to temper the data's variability. Such a frequency could arise from the natural resonance of the vehicles' suspension or from some other periodic perturbation resulting from on-road motion. The data was transformed into frequency space and various frequency filters were applied to test the data's response to frequency modulation. The relative amplitude of underlying frequencies are seen in *Figure 17*. The possible frequencies to sample are limited up to 10 Hz in accord with the Nyquist criterion. Low frequency amplitudes are abundant while higher frequencies are much less significant. A high pass filter removes the low frequencies and transforms the data back to its original state in *Figure 18*, clearly destroying original data quality. A low pass filter performs the inverse of the high pass, and the results are seen in *Figure 19*, but no significant difference between the low pass filtered data and original data was calculated. A band stop filter, where frequencies intermediate to the high and low filters were retained, was applied but again no significant difference was calculated.

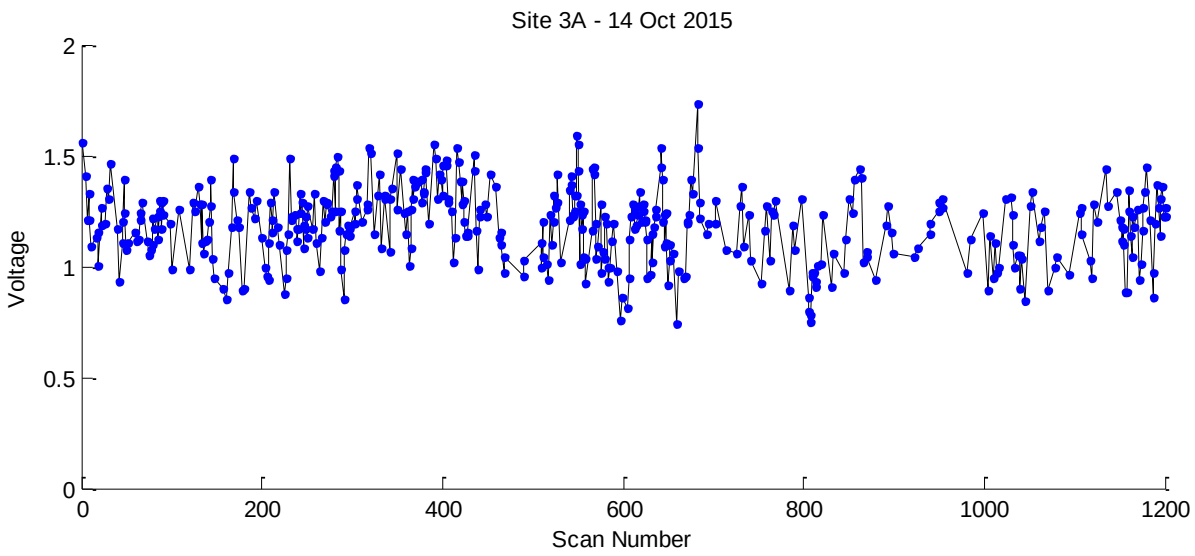


Figure 16: Data to analyze with Fourier technique.

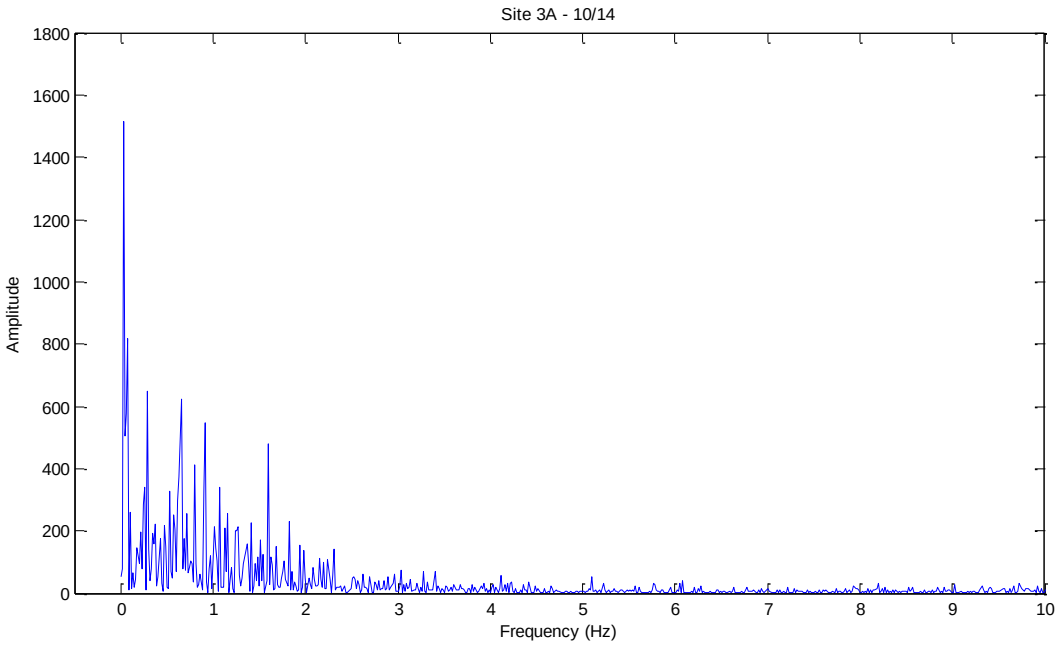


Figure 17: Frequency space analysis.

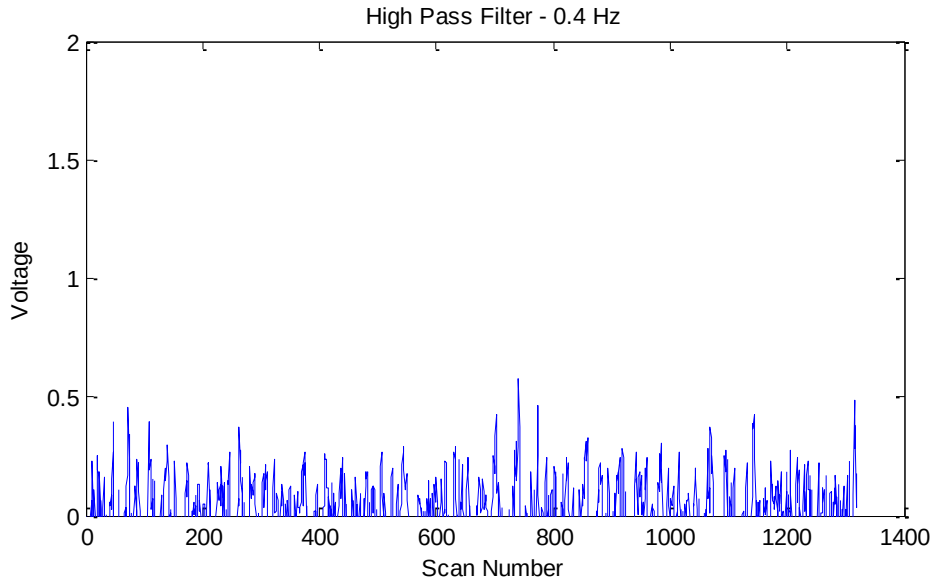


Figure 18: High pass filter Fourier analysis.

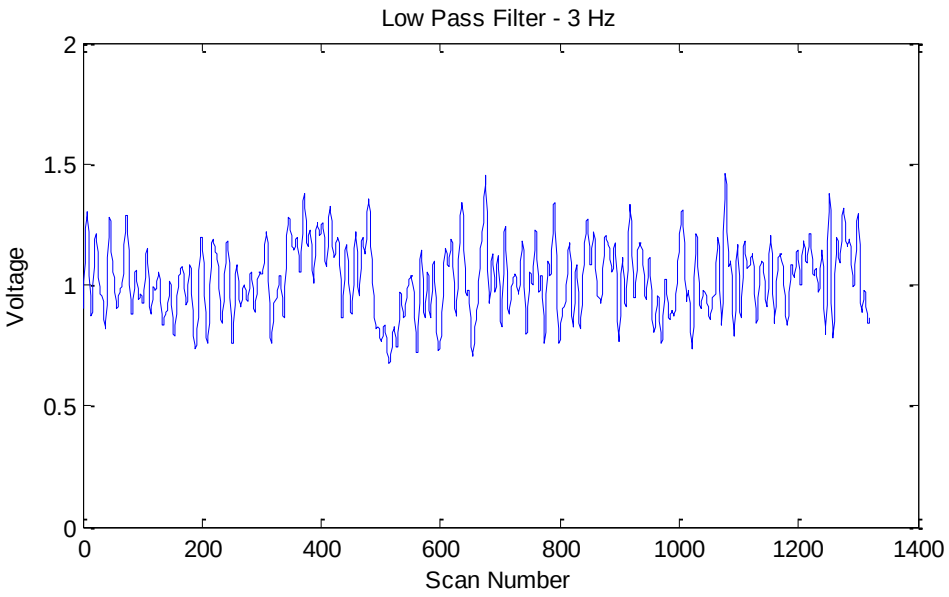


Figure 19: Low pass filter Fourier analysis.

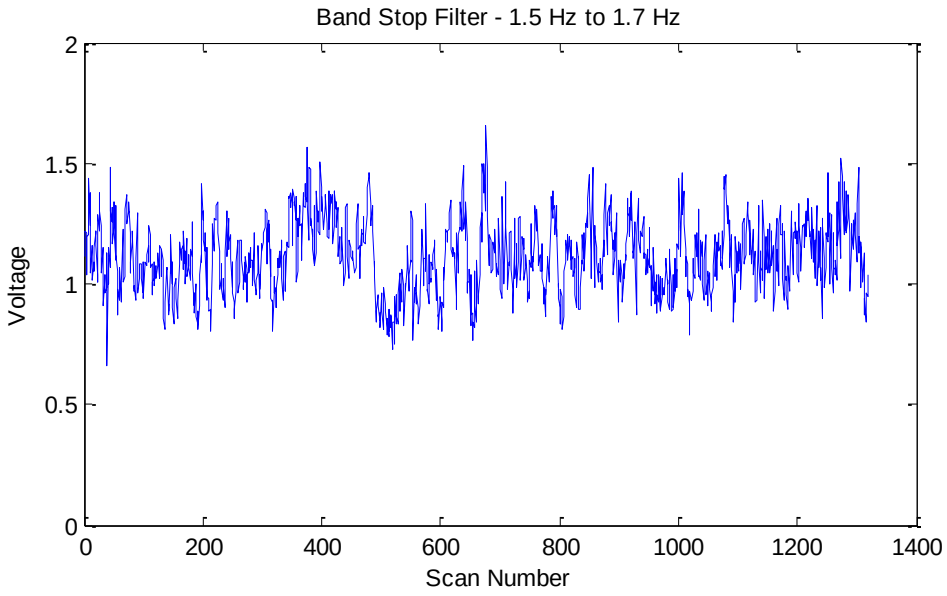


Figure 20: Band stop filter Fourier analysis.

### *4.3.4. Lateral Wander Correlation*

Effects of vehicle motion side to side during on-road collections introduce a distinct variability into the $R_L$ measurement, as discussed in Section 4.3.1. Retro-reflectivity readings collected when the stripe is in the center of the viewing window are different than measurements acquired when the stripe is toward the outside. Consecutive measurements of a given road section can lose repeatability solely due to the fact that lateral wander changes the value of measured $R_L$. A correlation is implemented in order to compensate for this effect. Data was taken in a manner shown in *Figure 21* and a resulting correlation was derived as shown in *Figure 22*. Incorporating this mitigation into the software reduced the data variability by 4.7%.

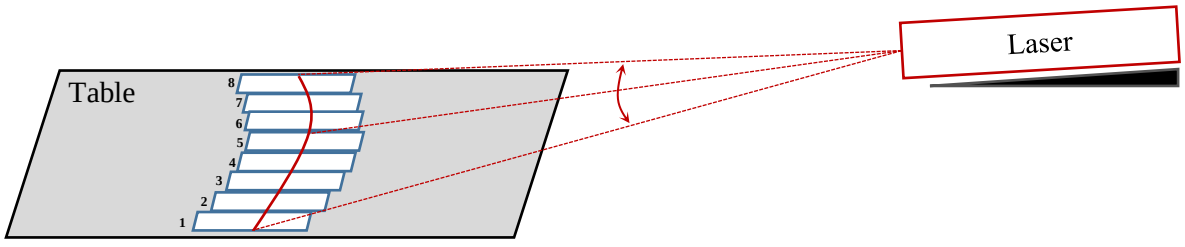


Figure 21: Lab setup for lateral correlation derivation.

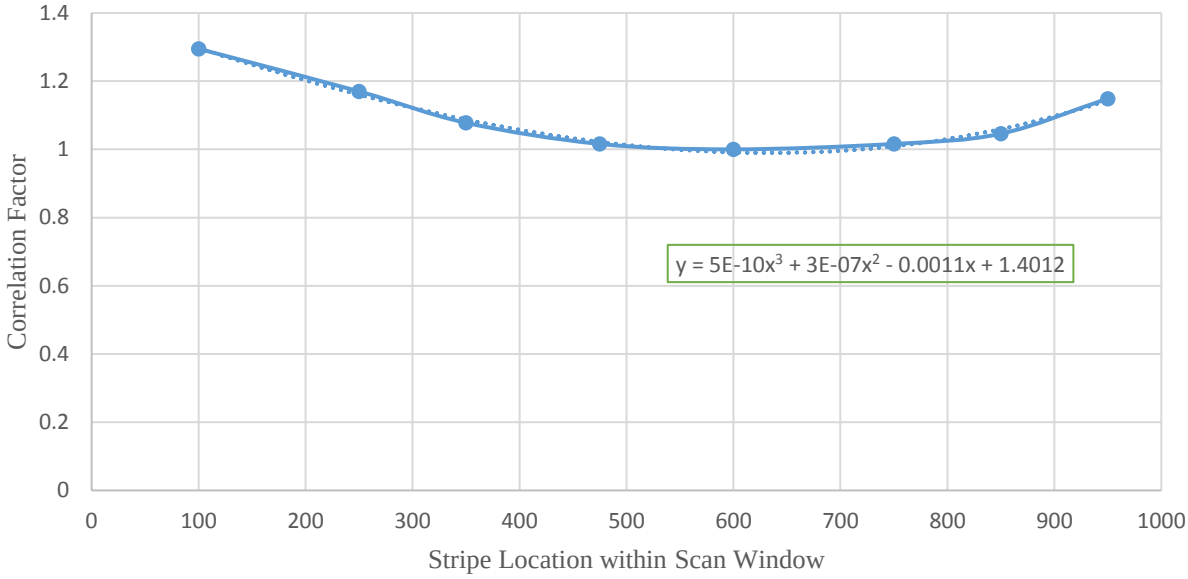


Figure 22: Curve fit establishing lateral correlation.

### 4.4. Implementation Software

The MRU is supplied by the manufacturer with control and data acquisition software. This software provides limited data and is difficult to modify to operator requirements. An alternative to the MRU control was developed as part of this effort, and the new software program is entitled Florida Retroreflectivity Software (FRS). FRS is a single application program with a drop down menu, conforming to conventional program design, thus eliminating any need for the operator to control low-level data processing subroutines or interface with programming languages. The operator can use the program nearly identically to the vendor's software with all the necessary input information and operational output data. Input data is entered by the operator from the drop down menu where information is organized into relevant categories. The front panel operator view can be seen in *Figure 23* along with a comparison shot of the vendor's program front panel. Drop down menu options can be seen in *Figure 24*.

In the vendor's software, superfluous data readouts are sprawled across the screen resulting in poor readability and distraction to the operator. FRS on the other hand simplifies data readouts by combining relevant information into a single pop up window, available from the drop down menu (*Figure 25*). From this window, information such as spinning mirror frequency, thermistor reading, and vehicle speed can be accessed quickly and easily.

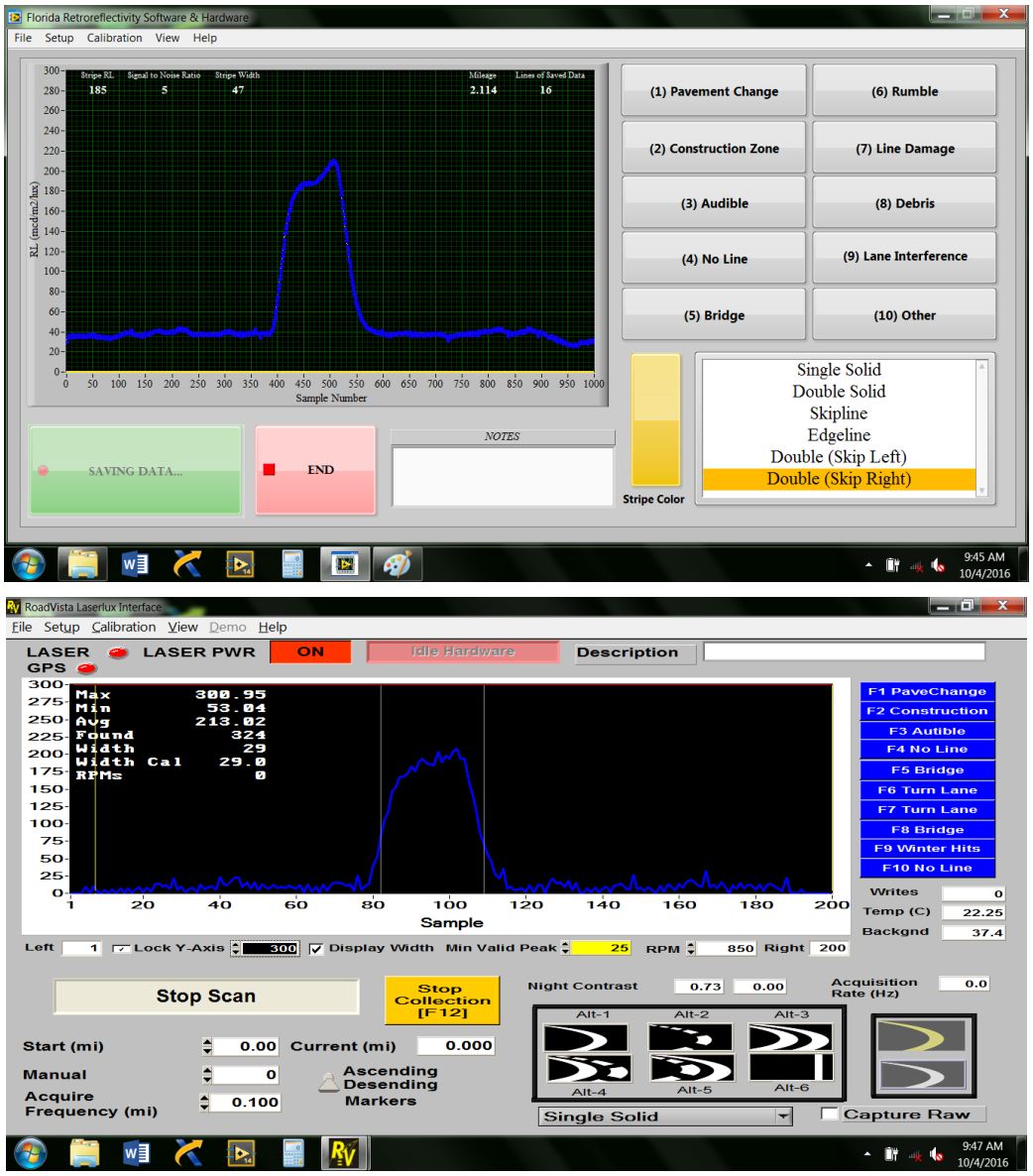


Figure 23: FRS (Top) and vendor software (Bottom) comparison.

A real-time display of processed data is available to the operator to check on-road measurements (*Figure 26*). The display is identical to the data being saved to the Excel file, allowing the operator to evaluate the quality of data collection at any point during the test. Tenth mile averages are included as well as relevant criteria such as event codes and stripe type. Making the Excel data available at any time during a test allows the operator to identify erroneous or unexpected data early in the testing and saves time if restarting the test is necessary. The vendor's software does not have this capability and makes the data available for evaluation only after the test is complete and the data is loaded into the Excel file.

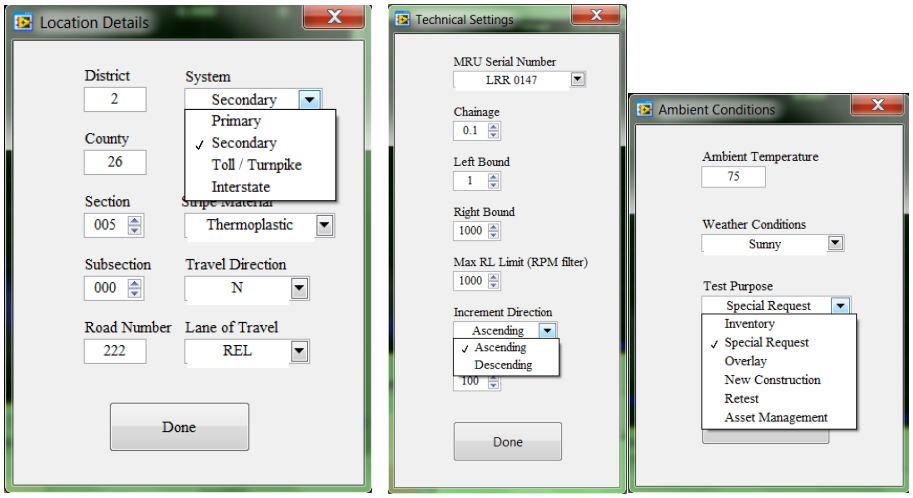


Figure 24: Drop down menu options.

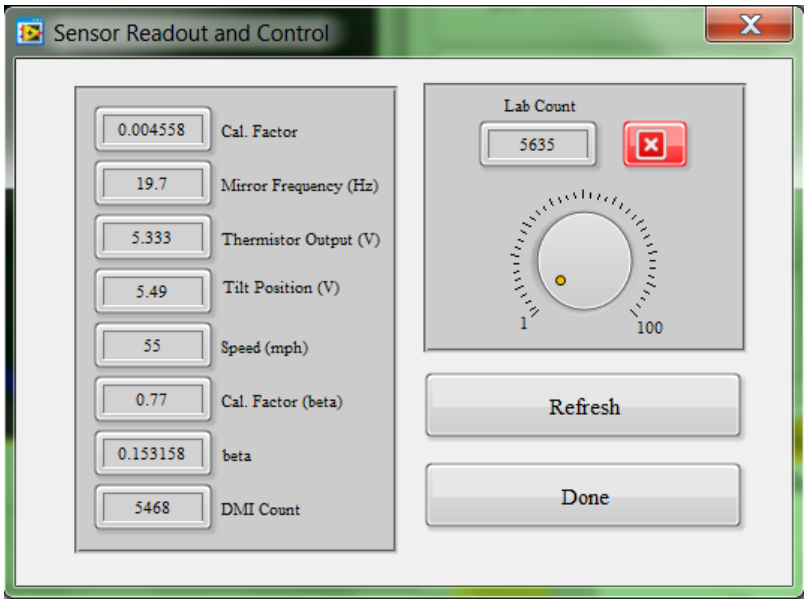


Figure 25: Sensor readout data.

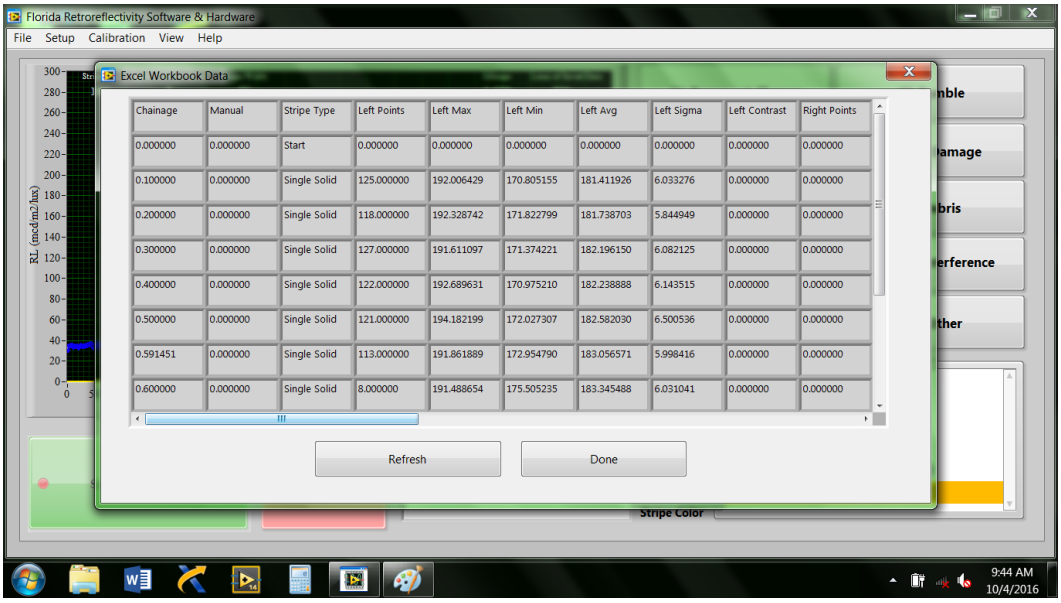


Figure 26: Real time data spreadsheet.

# 5. On-Road Testing and Debugging

## 5.1. Power Supply Inconsistency

Power is supplied to the MRU during on-road testing by the vehicle's 12 V system (battery and alternator). The quality of the power supplied was initially questioned in the investigation of an observed vertical offset as discussed in Section 5.3. For an MRU connected to the laboratory power supply (operates off wall power) and collecting data from a static test stripe, the average voltage data resembles that of *Figure 27*. However, it was observed that when the same stripe was measured from an MRU installed on the vehicle, the data loses significant quality. Further investigation identified the root cause to be thermoelectric cooler (TEC) operation. The change in data from a clean, steady signal in *Figure 27* to a rather erratic signal in *Figure 28* results in significant loss in data repeatability.

Improvement in the quality of the power supplied to the MRU was achieved by implementing a capacitive coupling which stores battery energy and removes the effects seen in *Figure 28*. However, this data indicates that power supply variations are not negligible and can have a significant negative effect on MRU data. Future modifications and improvements should pay attention to the consistency of on-vehicle power supply to ensure the quality of data.

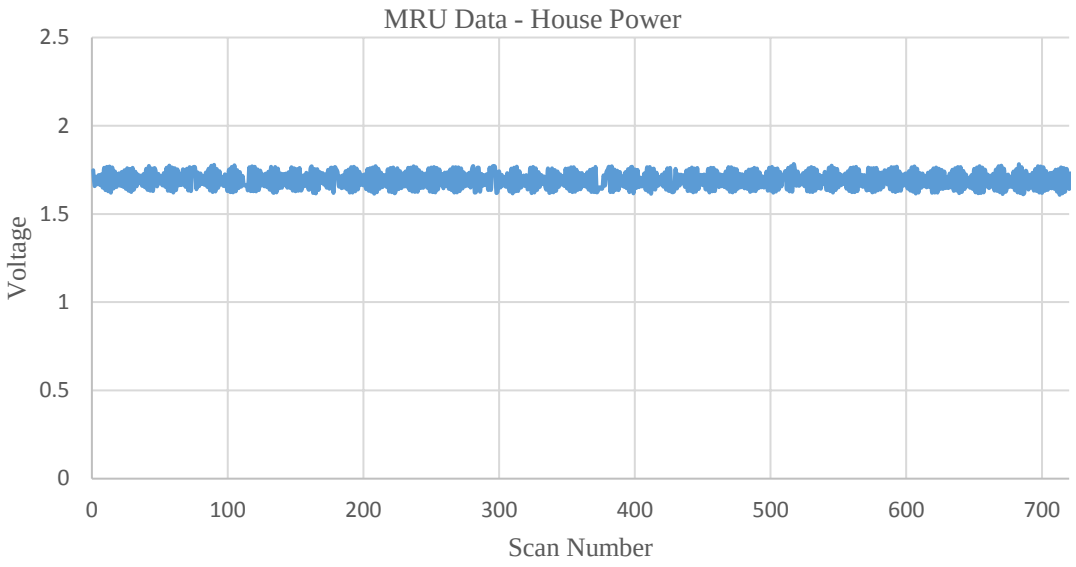


Figure 27: Data using stable house power supply.

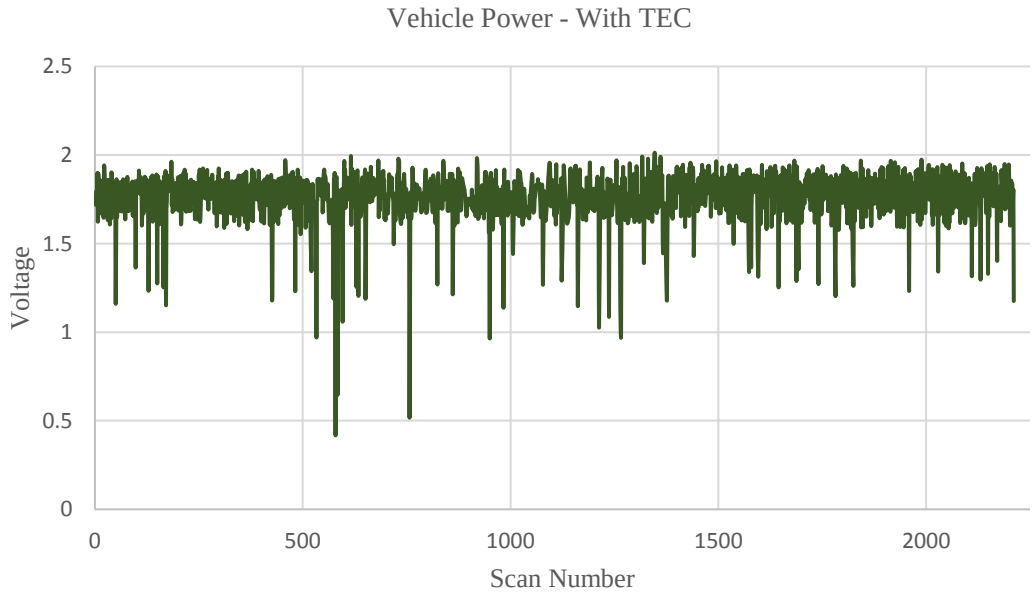


Figure 28: Data quality loss due to thermoelectric cooler.

### 5.2. Background Light Effects

Since the MRU operates by making a measurement of light incident upon a photodetector, any extraneous light will affect the measurement. The design of the MRU hardware includes two interference filters which ideally block all light that is not that of the laser (632.8 nm). The effect of background light on MRU performance was tested by the following two methods: by changing

the direction of sun light relative to the MRU and by testing during different levels of background light. The directional effect of the sun, specifically the orientation of the sun and the MRU, was tested by first testing the MRU in a stationary condition for 15 minutes while collecting data of the stripe reflectivity of a static test sample. The same stripe in the same position is measured again for 15 minutes, but with the MRU facing the opposite direction. The relative orientation of the MRU and sun changes how solar light reflects from the stripe and onto the MRU. The resulting change in measured voltage is shown in *Figure 29*, where the difference between the two data is 14.1%, a significant difference.

A second experiment was conducted where the orientation of the sun was fixed and the magnitude of the solar effect was adjusted by collecting data while the sample was in full sun and then alternatively shaded entirely. The difference between a stripe which is alternatively measured in full sun and shade was 4.4%, also a significant difference.

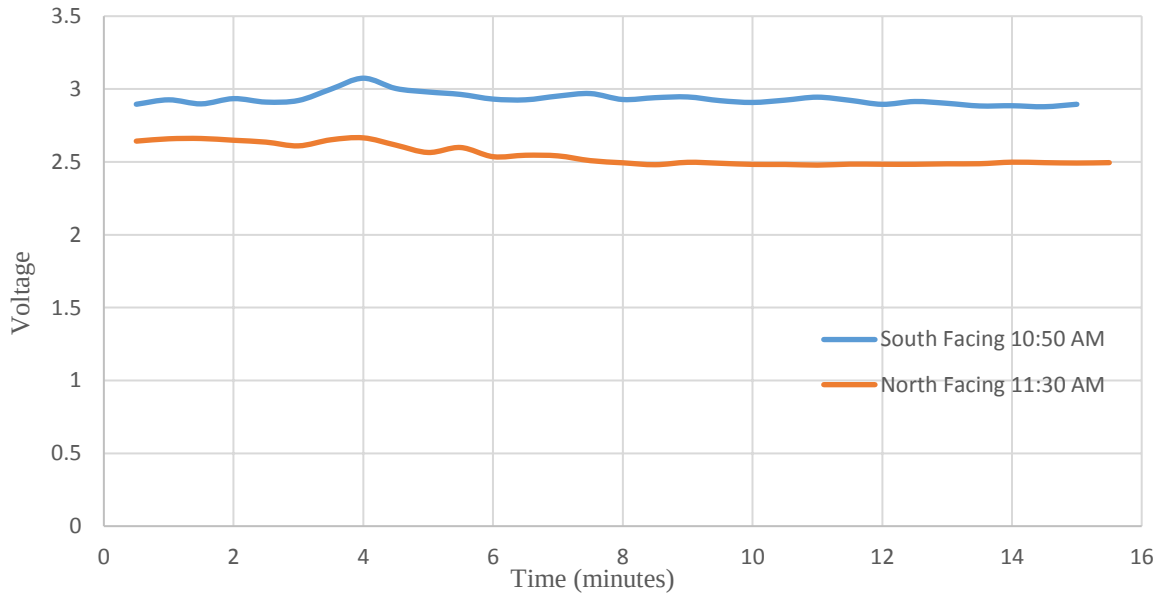


Figure 29: Effect of solar orientation.

### 5.3. Voltage Offset

A significant loss of repeatability in the data observed during on-road testing manifested itself as a voltage offset between consecutive runs (*Figure 30*). While the effect was observed on multiple occasions, the effect was not repeatable on a regular basis, further clouding the reasons for the offset. Several explanations such as temperature sensitive interference filters, power supply instability, and background light effects were all investigated in order to identify the root cause of the issue.

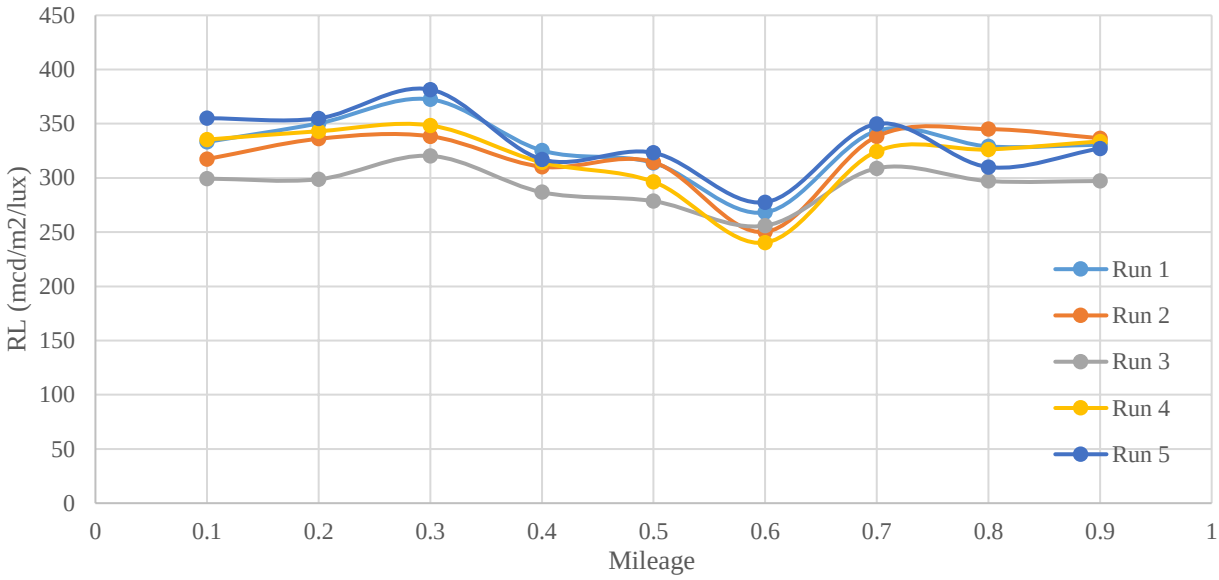


Figure 30: Example of vertical offset between runs.

One initial solution which mitigated the vertical offset was suspending the use of vehicle air conditioner. FDOT operators of the vehicle began this practice by noting that data repeatability was inferior if the MRU was attached to the side on which the AC condenser was located. It was inferred that the offset was partially due to condensed water dripping from the vehicle, falling onto the roadway, and splattering onto the MRU front glass. By deactivating the vehicle air conditioner, the problem was mitigated. Further designs may incorporate a drip catch or other mechanism to allow for simultaneous AC and MRU operation.

### *5.3.1. Histogram Analysis*

Data collected from precision sites often resembles that of *Figure 30* where there is unexplained variability over a single test site. Even significant differences between consecutive runs are not always well understood. One representation of data using histograms (*Figure 31*) was explored in hopes of discovering embedded information which can provide evidence toward the source of measurement variability.

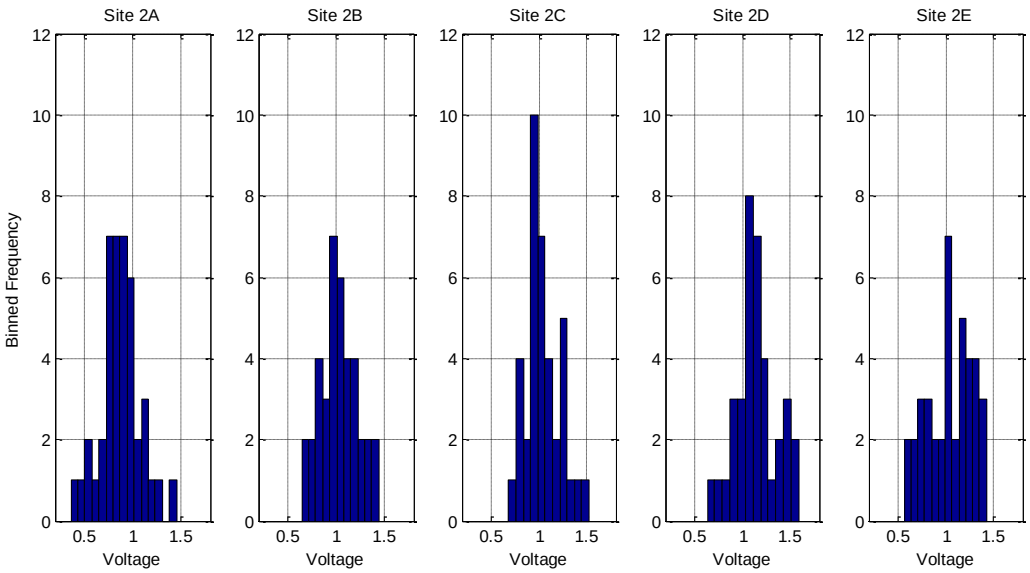


Figure 31: Histogram analysis.

Histogram analysis showed the spread of reflectivity data within a single tenth mile. While it is certain that between two consecutive runs that data collected by the MRU will be slightly different, the averages over that entire tenth mile should remain close. Histogram analysis indicates that the variability with data collected over the same tenth mile interval is not consistent but appears to be the result of several different simultaneous effects which result in unexplained variations between consecutive runs.

### 5.4. Spinning Mirror Assembly Effects

It was noted that in laboratory testing under static conditions the averaged stripe voltage for a given test stripe have a level of variability due to the wobble of the spinning mirror assembly. *Figure 32* illustrates the point by showing how these individual points vary in time while measuring an unchanging sample. The corresponding repeatability for spinning mirror variability is 8.6%. However, if the data is averaged over a large number of mirror cycles the repeatability is recovered. Relying on large amounts of data to average is critical to maintain reasonable repeatability. Future studies may need to consider the spinning mirror effect if higher degrees of precision is required for fewer data points.

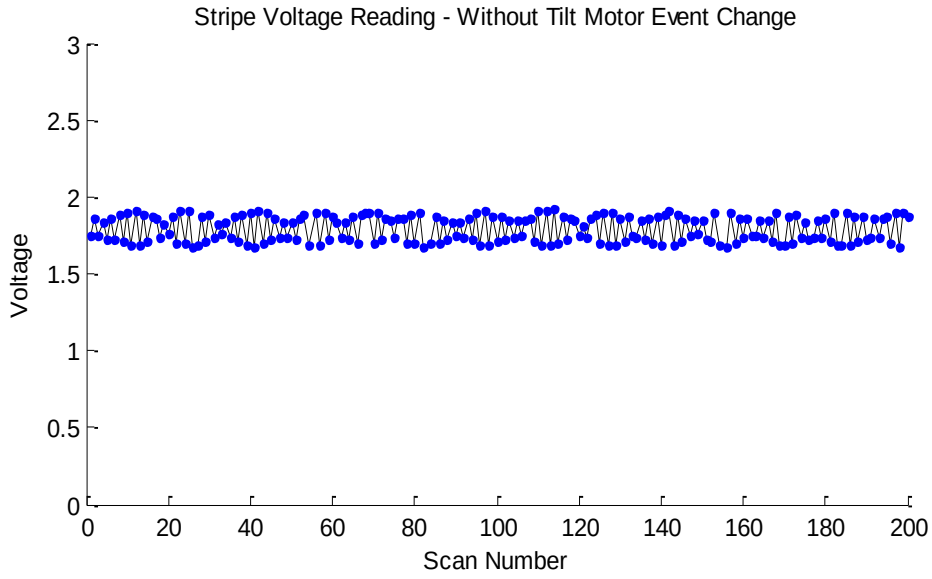


Figure 32: Variation due to spinning mirror instability.

## 6. Repeatability Study

Using FRS, on-road data was collected at a number of pre-selected sites. The sites are a combination of ideal precision sites (sites 1 – 5) and real-world sites which include dynamics such as intersections and vehicle speed changes (sites 6 – 8). Three consecutive runs were performed at sites 1 – 5 demonstrating average repeatability improvement over all five sites, see *Table 2*. *Figure 33* illustrates the consistency of data measured from these sites [1].

Data collected from sites 6 – 8 are characterized by realistic road conditions such as intersections and vehicle speed changes. Such inputs tend to drive repeatability upwards, as seen in *Table 3*. Note that run 1 was omitted from the data set because it was affected by rain. Upon inspection of the data, the loss in repeatability appeared to be the result of vertical offsets between runs, as seen in *Figure 34*. Such vertical offsets are typically the result of some constant or predictable factor and can be mitigated once the root cause is identified. It should be noted that runs 2 – 4 are the most repeatable and these three runs were collected consecutively on a single day. Run 5 was collected the next day in overcast conditions (low background light) and run 6 was collected in sunny conditions.

Table 2: Summary of repeatabilities at sites 1-5 (3 runs).

| Site Number | *Vendor Software* | | *FRS* | |
|---|---|---|---|---|
| | Std. Dev. ($R_L$) | d2s% | Std. Dev. ($R_L$) | d2s% |
| 1 | 7 | 5.9% | 5 | 4.3% |
| 2 | 5 | 5.3% | 4 | 5.0% |
| 3 | 6 | 8.4% | 2 | 2.3% |
| 4 | 3 | 4.8% | 5 | 7.4% |
| 5 | 6 | 5.0% | 6 | 6.3% |
| Avg. | 5 | 5.9% | 4 | 5% |

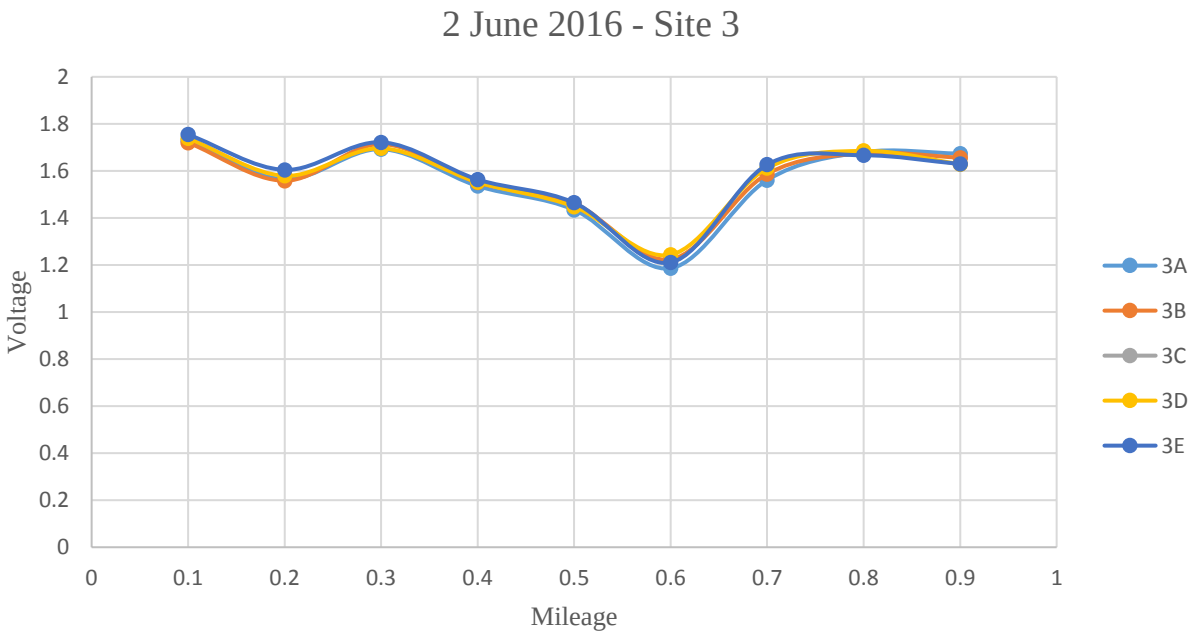


Figure 33: Data from precision site 3 exhibiting superb repeatability.

Table 3: Data collection at sites 6-8 (5 runs).

| Site Number | *Vendor Software* | | *FRS* | |
|---|---|---|---|---|
| | Std. Dev. ($R_L$) | d2s% | Std. Dev. ($R_L$) | d2s% |
| 6 | 19 | 22.0% | 18 | 25.8% |
| 7 | 21 | 23.0% | 22 | 25.9% |
| 8 | 23 | 23.7% | 15 | 19.7% |
| Avg. | 21 | 22.9% | 18 | 23.8% |

Data from sites 6 – 8 exhibited vertical offsetting resulting in loss of repeatability. It is proposed that the root cause of the vertical offsetting is the deficiency of the MRU hardware, specifically the interference filters. The interference filters are designed to pass only the frequency of light characteristic of the laser, but background ambient light may not be satisfactorily filtered out. As seen in *Figure 34*, peaks and trends of all 5 runs are similar and are only vertically shifted (probably due to changes in ambient light).

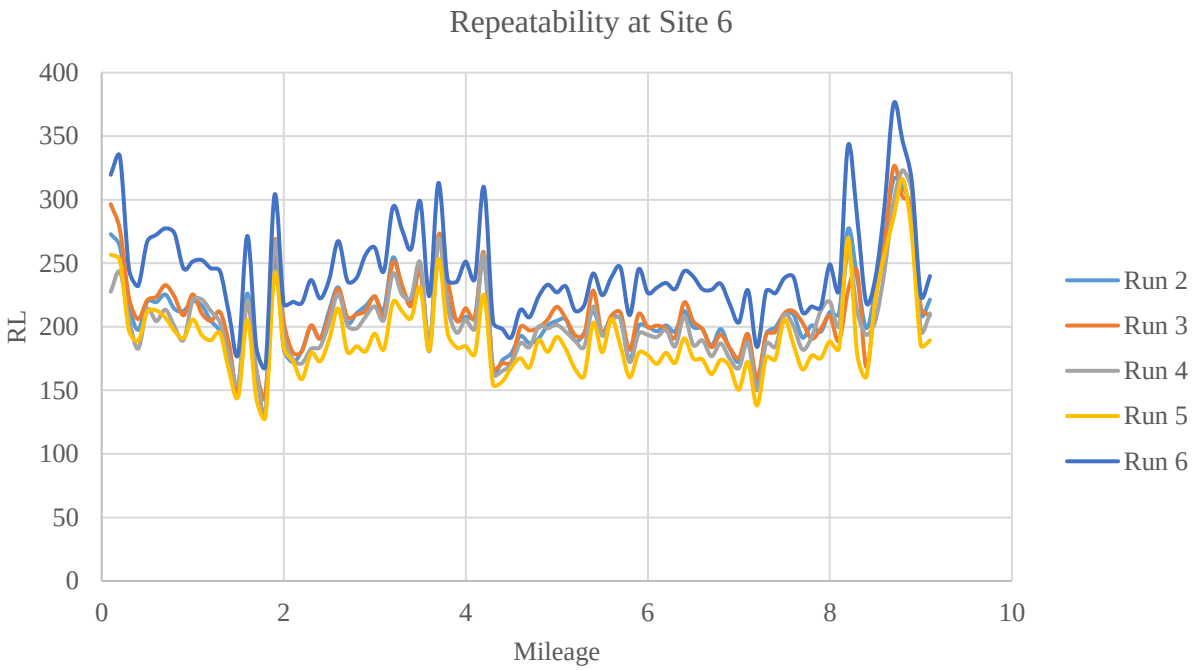


Figure 34: Vertical offsetting at site 6.

Given the potential impact of changes in ambient light during runs 5 and 6, the repeatability for the data set at sites 6 – 8 was recalculated for only runs 2 – 4, where ambient conditions changed minimally. The results are displayed in *Table 4*. Using this subset, the repeatability improves significantly and demonstrates improved performance with respect to the vendor's software. The data indicates that ambient light conditions play a significant role in affecting the tenth mile averaged data, specifically by offsetting the data vertically either upward or downward.

Additional analysis supports the hypothesis that background light directly effects the measured $R_L$. For example, additional data from Site 7 was collected independently of the repeatability study. The upper graph of *Figure 35* shows four data sets taken at two different times over two consecutive days which had similar atmospheric conditions. The two times of day were such that the solar orientation changes significantly over two hours, i.e. in the morning time. Note that the data at the same time of day (9 AM and 11 AM) is more self-consistent than data taken the same day but at different times (Jan 11 and Jan 12). Additionally, the vertical offset appears to switch mid-run, likely due to opposite changes in sunlight conditions between runs i.e. one part of roadway became shaded while another became exposed to direct sunlight.

Table 4: Site 6-8 repeatability calculated under consistent ambient conditions (Run #2-4)

| Site Number | *Vendor* | | *FRS* | |
|---|---|---|---|---|
| | Std. Dev. ($R_L$) | d2s% | Std. Dev. ($R_L$) | d2s% |
| 6 | 16 | 18.6% | 6 | 7.8% |
| 7 | 21 | 23.4% | 13 | 14.8% |
| 8 | 22 | 22.9% | 12 | 15.6% |
| Avg. | 20 | 21.6% | 10 | 12.7% |

The mid-run vertical shifting which appears in upper graph of *Figure 34* correlates well with the similar mid-run shifting of the background $R_L$. This background not only includes the $R_L$ of the pavement itself (quantity of laser light retro-reflected to the MRU photodetector), but also any ambient solar light which may reflect towards the MRU. If the ambient light did not affect background voltage, than $R_L$ of the surrounding pavement should remain unchanged at different times of the day. This data is strong proof that the level and direction of ambient light has a strong influence on MRU performance. Given that the effect of ambient light should be minimized by the interference filters but is not, more testing and effort to characterize the performance of this MRU sub-system hardware is needed. Once the hardware performance is characterized, including the effect of aging on interference filter performance, mitigation strategies can be incorporated into the FRS software.

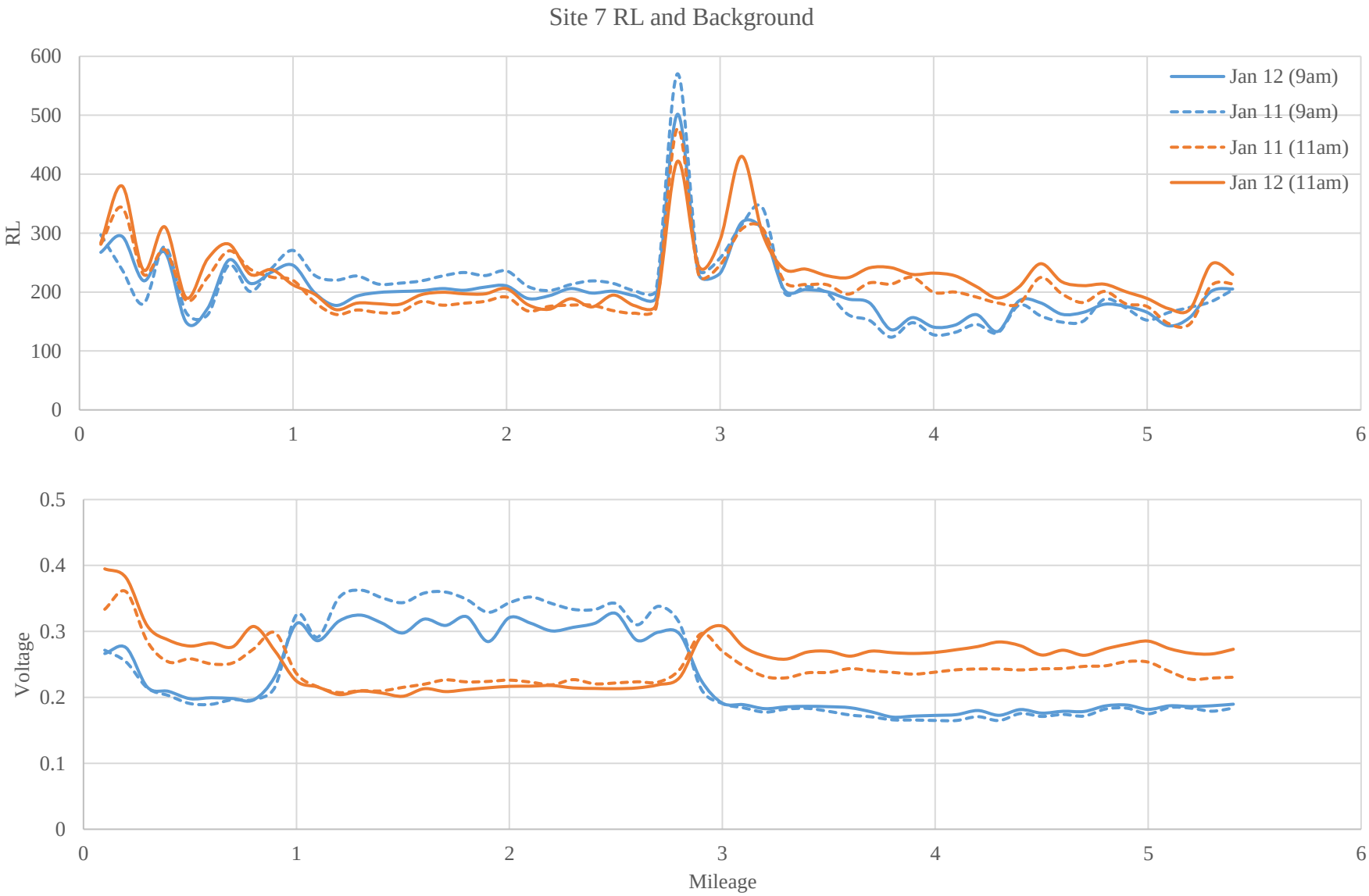


Figure 35: Retroreflectivity and background voltage correlation.

While the MRU is designed to sufficiently mitigate ambient light via the interference filters, these filters tend to lose efficacy over time and allow increasing amounts of ambient light to be measured. The effects of interference filter degradation over time needs further investigation to evaluate how and when the interference filters fail, and at what point they need to be replaced to provide accurate data.

However, immediate response and partial mitigation of ambient effects can be accomplished with a background light correlation. This correlation will use background signal data to correct vertical shifting of $R_L$ data. As seen in *Figure 34*, background signal behavior corresponds to similar shifting in the tenth mile average at identical mileage.

## 7. Conclusions and Future Work

A new software application, Florida Retroreflectivity Software (FRS), has been successfully developed that provides complete MRU control as well as providing an easy-to-use operator interface[2]. Substantial testing was undertaken to characterize the MRU response to a line stripe and algorithms were developed to ensure that only data that is truly representative of the stripe is used to evaluate the retro-reflectivity. Testing has shown improvement over the Vendor-supplied software. At sites 1 – 5, FRS demonstrated 0.9% average improvement in repeatability as calculated by the d2s% method. At sites 6 – 8, an 8.9% improvement was observed when data was collected under similarly consistent background light conditions.

The FRS software provides much more data to the investigators that the Vendor-supplied hardware, and as a result, it has been determined that data collected under conditions of variable ambient light conditions showed vertical shifting between runs and was characterized by inferior repeatability. The background $R_L$ reading correlates to the vertical shifting, and such background $R_L$ is due to a combination of pavement $R_L$ and solar background light. The MRU is designed to mitigate the effect of background solar light by the interference filters internal to the MRU hardware, but testing showed that hardware performance is insufficient to achieve improved levels of repeatability under ambient light conditions. Interference filter quality degrade with age and further testing is needed to characterize this effect.

# Glossary

| | |
|---|---|
| candela | Base unit of luminous intensity as weighted to the human eye<br>Watts per steradian |
| COV | Coefficient of variation<br>Calculated as the standard deviation divided by the mean |
| DAQ | Data Acquisition |
| d2s (%) | ASTM standard for maximum difference between two test results<br>Calculated by multiplying the COV by the factor $1.96\sqrt{2}$ |
| LabVIEW | Laboratory Virtual Instrumentation Engineering Workbench |
| lumen | A measure of total quantity of visible light emitted by a source<br>1 lumen = 1 candela $\times 4\pi$ steradians |
| lux | SI unit of lumens per square meter |
| NI | National Instruments |
| mcd | One thousandth of one candela |
| MATLAB | Matrix Laboratory |
| MRU | Mobile Retroreflectivity Unit |
| $R_L$ | Derived unit of retroreflectivity<br>1 $R_L$ = 1 mcd/lux/$m^2$ |
| RPM | Raised Pavement Marker |

# References

[1] FDOT drive address for reported data: Q:\Pavement Systems\NDT\MRU\UNF contracts\MRU Algorithm - UNF\Field Data\Repeatability Study

[2] FDOT drive address for FRS operation guide: \\SM.dot.state.fl.us\MappedDrives\Pavement Systems\NDT\MRU\UNF contracts\MRU Algorithm - UNF\Tasks\Task Completion Reports\Task 6